TELKOMNIKA, Vol.17, No.6, December 2019, pp.2713~2721
ISSN: 1693-6930, accredited First Grade by Kemenristekdikti, Decree No: 21/E/KPT/2018
DOI: 10.12928/TELKOMNIKA.v17i6.12087

Enhancement algorithm for reverse loop technique on planar reverse loop antenna

Mohamad Harris Misran*[1], Sharul Kamal Abdul Rahim[2], Maizatul Alice Meor Said[3], Mohd Azlishah Othman[4]
[1,2]Wireless Communication Centre (WCC), Faculty of Electrical Engineering,
Universiti Teknologi Malaysia, 81310 UTM Skudai Johor, Malaysia
[1,3,4]Fakulti Kejuruteraan Elektrik dan Kejuruteraan Komputer, Universiti Teknikal Malaysia Melaka,
Hang Tuah Jaya, 76100 Durian Tunggal, Melaka, Malaysia
*Corresponding author, e-mail: harris@utem.edu.my[1], sharulkamal@fke.utm.my[2], maizatul@utem.edu.my[3]

Abstract

Finding a trade-off balance between wireless transfer efficiency (WTE) and distance is a key issue in wireless energy transfer (WET). This paper presents a method of reducing the radical alteration in WTE versus distance, by using a reverse loop technique on planar reverse loop antenna (PRLA). The design focuses on 13.56 MHz Near Field Communication (NFC). The first stage uses mathematical modelling, based on an analytical approach, to determine the size of the reverse loop using Matlab. The proposed model predicts the size of the reverse loop to stabilize the WTE at a closer distance. Next, full-wave electromagnetic simulations are applied, using the computer simulation technology (CST) MICROWAVE STUDIO®, to determine the WTE effect with distance changes with mismatch condition. Planar loop antennas (PLAs) are fabricated on glass-reinforced epoxy laminated sheets (FR4). A validation of the simulation result in a real test scenario, using these PLAs and PRLA, confirms a stability enhancement in WTE at closer distance using the reverse loop technique, compared to conventional designs.

Keywords*: near field communication (NFC), planar loop antenna (PLA), planar reverse loop antenna (PRLA), wireless energy transfer (WET), wireless transfer efficiency (WTE)*

1. Introduction

With the evolution of high-end technology, portable devices have become widely used. Usually, these devices require power from rechargeable batteries to enable mobility. The batteries only support these devices for limited durations, after which they require recharging using wired power delivery mechanisms. Consumers usually need to wait for the completion of the charging process before the devices can be used wirelessly. In its mooted counteraction of this problem, wireless energy transfer (WET) has garnered significant research interest. However, even with the latest technologies, there are obstacles to be overcome before the full commercialization of WET can be implemented [1].

Inductive coupling of WET has attracted a great deal of attention, due to its simplicity and safety. It is already used in technologies such as RFID and NFC [2]; NFC-enabled smartphones are even now employing inductive coupling for data transfer in contactless transactions at 13.56 MHz [3]. Theoretically, NFC can also be used to transfer energy between devices using inductive coupling at a resonant frequency as shown in Figure 1.

There have been improvements in the performance of inductive coupling and strong magnetic coupling WET schemes [4-6]. However, as demonstrated in many studies, the wireless transfer efficiency (WTE) is reduced greatly with altered distances [6-11]. In order to increase the insensitivity to the distance of the transmitting and receiving antennas, a handful of techniques has been developed, such as using a loaded capacitor or applying more than two coils in a system [6, 11, 12].

Coupling coefficient is directly proportional to mutual inductance; M. M value strongly depends on the distance between the antennas. In short, closer distance will generate higher M than farther distance. Both antennas are perfectly matched at operating distance for optimum resonant effect. However, the WTE will radically drop when the transmitter and receiver become closer. This phenomenon happens because of frequency splitting condition caused by coupling

Received December 18, 2018; Revised January 21, 2019; Accepted March 12, 2019

coefficient inflation [13]. In order to maintain a constant transfer within the over-coupled region, some researchers proposed dynamic impedance matching arrangements to either track the resonance frequency [14-17] or adaptively impedance match to maintain a stated frequency [18]. These impedance matching arrangements were implemented using either lumped reactance [14, 19, 20] or tuning algorithms in controllers [21–23]. An alternative arrangement, however, is to control the range-profile of the mutual inductance within the over-coupled region.

Besides, optimal load resistance value existed, with which the coupling efficiency can be maximised [24]. To achieve this, the resonant capacitor at the load side was replaced by a more complex impedance matching network in [16, 25]. This matching network tuned the receiver coil and transformed the load resistance value into one that is optimum. The matching network was also introduced into the source side in [25-27]. In [25], the matching network design was integrated into WET system and displayed a good performance. Matching network can be designed to maximise the output power for transfer efficiency.

This paper focuses on 13.56 MHz WET, in order to take advantage of the fact that almost all mid- and high-end smartphones are already NFC-enabled. The reverse loop technique is used to stabilize the WTE when the distance between both antennas is shorter than optimum operating distance, without any further system adjustment. The M produced is controlled by introducing a reverse loop into a planar loop antenna (PLA) to minimize the radical changes in WTE with distance variance. This method yields the development of the planar reverse loop antenna (PRLA).

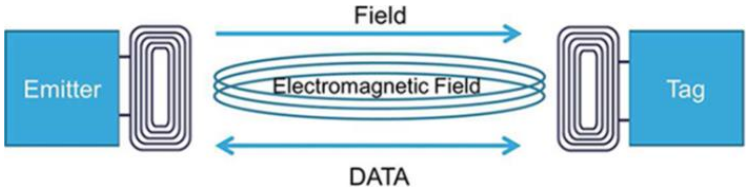

Figure 1. NFC transmission system [2]

2. Antenna Design

The inductive coupling link consists of two antennas with separate external matching circuits. Each matching circuit uses parallel and serial capacitors to tune the antennas for maximum WTE at the operating frequency. The antennas are designed to be square in order to fit into mobile phones, thereby optimizing the available area. The PLAs are single square loops, as shown in Figures 2 (a) and (b). Their side-lengths are set at 60 mm and 40 mm for the transmitter and receiver, respectively, for an operating distance d of 50 mm.

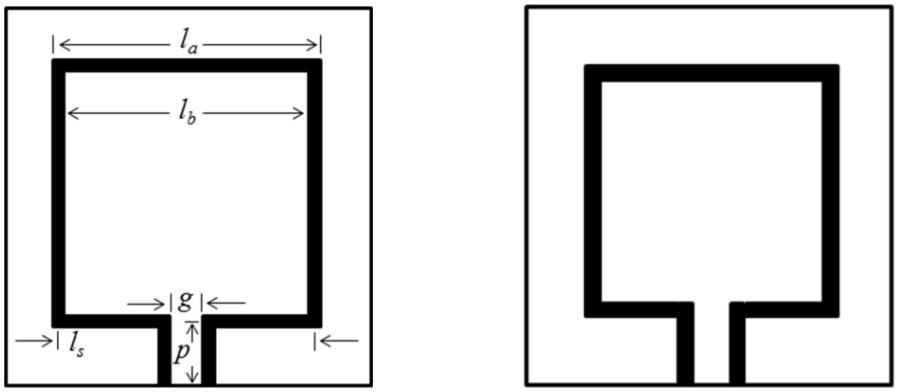

(a) (b)

Figure 2. (a) Transmitter PLA and (b) receiver PLA

A coupled pair of one-turn square loops in a wireless energy transfer link can be illustrated in a simplified equivalent circuit, as shown in Figure 3 [28]. The inductance of each PLA can be calculated using (1), also stated in [29]:

$$L_{TX,RX} = 0.635\mu l_x \left[\ln\left(\frac{2.07}{l_y}\right) + 0.18l_y + 0.13{l_y}^2\right] \quad (1)$$

where μ is the conductor (copper) permeability, and

$$l_y = \frac{l_a - l_b}{l_a + l_b} \quad (2)$$

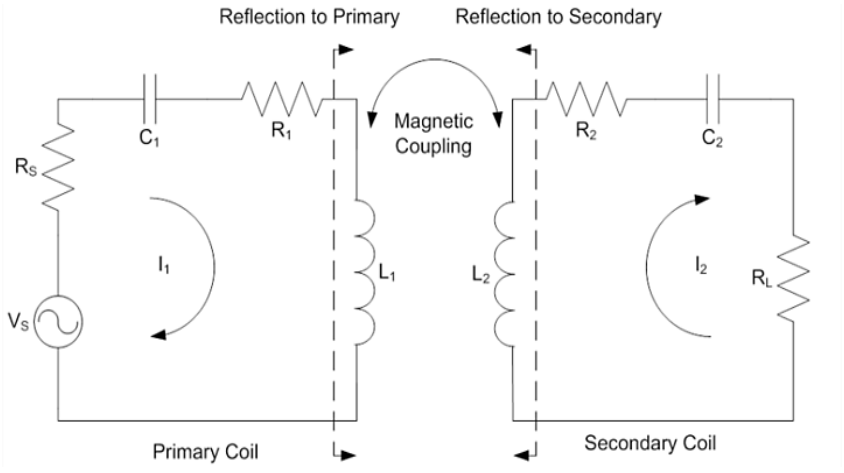

Figure 3. Equivalent circuit for antennas [28]

The average side length of the PLA is given by

$$l_x = 0.5(l_a + l_b) \quad (3)$$

with l_a and l_b denoting the largest and smallest side lengths, respectively. Taking the skin effect into consideration, the resistance of the PLA, R at f = 13.56 MHz, can be computed as:

$$R = \frac{\rho l}{4A_r\delta}\left(\frac{t}{1 - e^{-\frac{t}{\delta}}}\right) \quad (4)$$

$$\delta = \frac{\sqrt{\rho}}{\sqrt{\pi f \mu_o}} \quad (5)$$

where ρ is the resistivity of copper (1.7×10^{-8} Wm), A is the cross-sectional area of the loop and l is the total length of the PLA. t is the thickness of the conductor. A_r and l can be determined by using

$$A_r = w \times t \quad (6)$$

$$l = 4l_s - g + 2p \quad (7)$$

where w, l_s, g and p are the width, side length, gap length and port line length of the conductor respectively.

The WTE of the established link is calculated as [11]:

$$\eta = \frac{E}{\left(1+\sqrt{1+E}\right)^2} \tag{8}$$

$$E = k^2 Q_{TX} Q_{RX} \tag{9}$$

where Q_{TX} is the quality factor of the transmitting antenna and Q_{RX} is the quality factor of the receiving antenna; both are defined as

$$Q_{RX} = \frac{2\pi f\ L_{RX}}{R_{RX}} \tag{10}$$

$$Q_{TX} = \frac{2\pi f\ L_{TX}}{R_{TX}} \tag{11}$$

k is the coupling coefficient between both antennas and can be determined using:

$$k = \frac{M}{\sqrt{L_{TX} L_{RX}}} \tag{12}$$

the mutual inductance between both antennas, *M*, can be obtained using [29]:

$$M = \frac{\mu_o \pi X^2 Y^2}{2(X^2+Y^2+d^2)^{\frac{3}{2}}}\left(1+\frac{15}{32}\gamma^2+\frac{315}{1024}\gamma^4\right)\left(\frac{4}{\pi}\right)^{1+\frac{r_{min}}{r_{max}}} \tag{13}$$

$$\gamma = \frac{2X^2Y^2}{X^2+Y^2+d^2} \tag{14}$$

r_{min} and r_{max} are the corresponding smaller and larger side lengths of the square antennas, respectively. Here, *X* is the half side length of the transmitter antenna and *Y* is the half side length of the receiver antenna. *d* denotes the distance between the transmitter and receiver of the PLA system.

In terms of mutual inductance between transmitter and receiver PLA, M is inversely proportional to the distance, as shown in Figure 4. In theory, high values of M will produce high WTE; however, this is only true if both PLAs are perfectly matched. In fixed matching circuits for inductive WET, the highest WTE will be obtained at a matching operating distance, which in this case is 50 mm. Deviation from this operating distance will greatly reduce the WTE of the system. Further distance from the operating point will reduce M value, also causing WTE reduction.

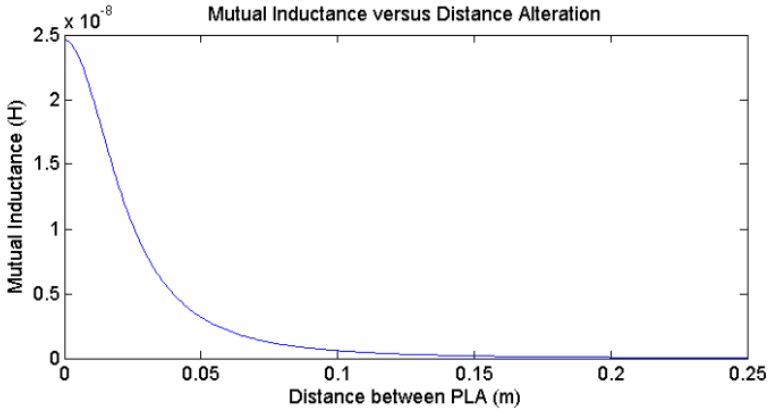

Figure 4. Mutual inductance, M versus distance between PLAs

Meanwhile, a closer distance from the operating point will increase the *M* between PLAs and create the over-coupling condition, as characterized by frequency splitting [13]. The over-coupling phenomena will decrease the WTE greatly, even when *M* is high at that point. In theory, the WTE can be stabilized by maintaining a constant M, irrespective of the distance. This can be achieved by introducing a reverse loop in the transmitter antenna, producing a PRLA, as shown in Figure 5 (a). The receiver antenna will be using initial single square loop antenna as presented in Figure 5 (b). This reverse loop will generate an opposite M, as shown in Figure 6. The net result will be a reduction in the alteration of *M* as the coupled antennas are brought closer together.

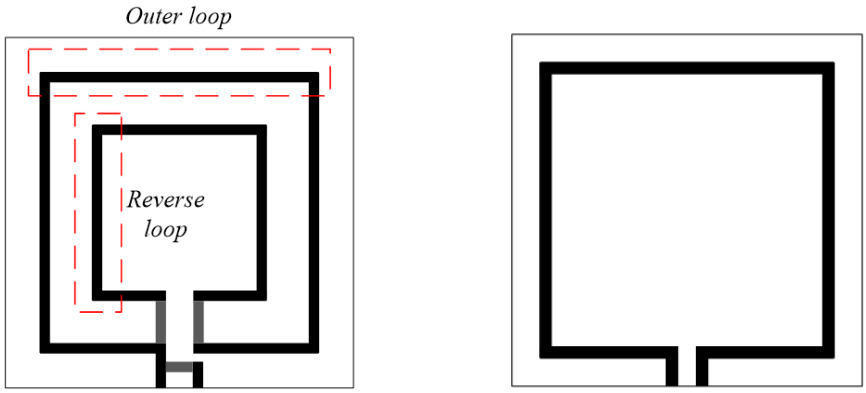

(a) (b)

Figure 5. (a) Transmitter PRLA and (b) receiver PRLA

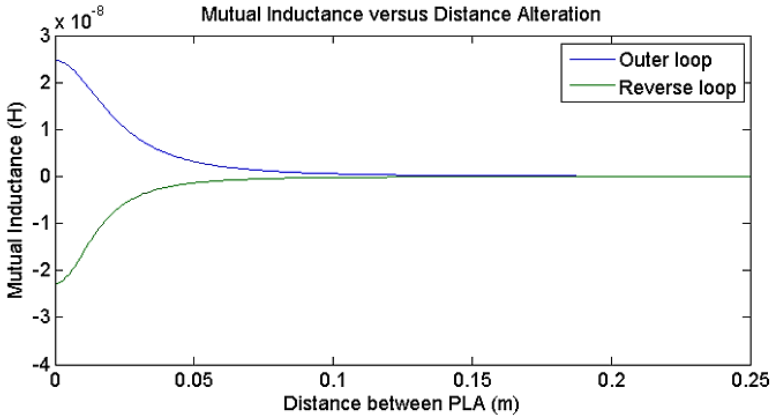

Figure 6. Mutual inductance, M versus distance between PRLAs

The first stage in obtaining the side length of the reverse loop requires the choice of two points of distance. The first point is an optimum operating distance, while the second is a closer distance than the former. Based on (13), maintaining the value of M at these two points will result in a stable WTE. The size of the reverse loop to maintain a constant M at both points can be obtained by solving (15). Matlab is used to solve the proposed equation.

M1,2 are calculated using:

$$M_{1,2} = \frac{\mu_o \pi A_{1,2}^2 B_{1,2}^2}{2\left(A_{1,2}^2 + B_{1,2}^2 + d_{1,2}^2\right)^{\frac{3}{2}}} \left(1 + \frac{15}{32} + \frac{315}{1024}\gamma_{1,2}^4\right)\left(\frac{4}{\pi}\right)^{1+\frac{r_{min}}{r_{max}}} \quad (15)$$

$$\gamma_{1,2} = \frac{2A_{1,2}^2 B_{1,2}^2}{A_{1,2}^2 + B_{1,2}^2 + d_{1,2}^2} \quad (16)$$

where A1,2, B1,2 and d1,2 are the half-side length of the transmitter, the half-side length of the receiver and the distance between PRLAs at different points, respectively. If A1, B1, d1, A2 and d2 are known, the optimum size of the reverse loop side length, B2 can be calculated. The calculated value of B2 is an optimum value of reverse loop side length that produces highest and most stable WTE at a distance between antennas closer than matching distance.

To tune the system for optimum performance at f = 13.56MHz, both PLAs and PRLAs were matched to 50Ω impedances using external capacitor networks, as shown in Figure 6. Full-wave simulations were carried out in CST to ascertain the effect on WTE with distance. The antennas were then fabricated to validate the simulated results.

3. Results and Analysis

Simulated antennas are matched using Mini Match matching technique in CST. Two capacitors are used at each antenna to eliminate the reactance component and get a resonance at 13.56 MHz, as shown in Figure 3. This matching stage is very important to ensure the maximum possible output power will be delivered. The fabricated transmitter's PLA and PRLA are shown in Figure 7, with the matching circuit shown in the inset. The capacitance values are shown in Table 1, while Figure 8 shows the lab measurement setup.

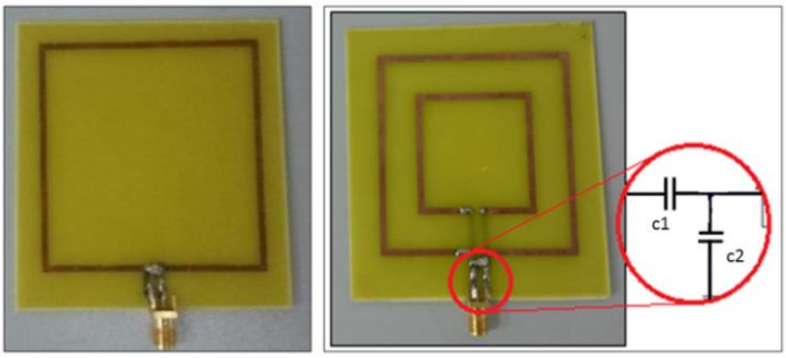

Figure 7. Fabricated PLA and PRLA

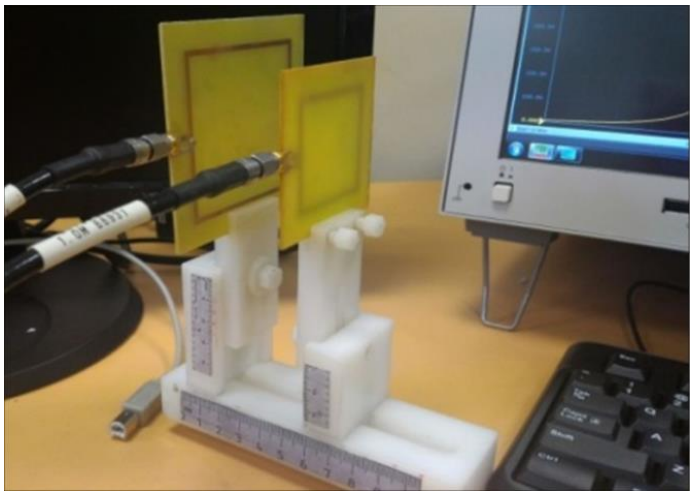

Figure 8. Measurement setup in lab using vector network analyser

Table 1. Capacitor values for matching circuit

Capacitor	PLA Value (pF) CST	PLA Value (pF) Actual	Capacitor	PRLA Value (pF) CST	PRLA Value (pF) Actual
C_1	74.5	75	C_1	52.58	52
C_2	650.3	651	C_2	541	545
C_3	1085.8	1090	C_3	1117	1120
C_4	104.9	105	C_4	69	68

The M of the system using PRLA is shown in Figure 9. Even though the PRLA has a lower M compared to the PLA, the M for the PRLA loop is much more stable over distance. This ensures the reduction of the over-coupling effect at closer distances; accordingly, frequency-splitting phenomena can be minimized. The WTE alteration, with shorter coupling distances than the matching distance, is thus reduced.

In Figure 9, the total M produced by the PLRA is shown. Total M is decreased because the reverse loop in PRLA introduced negative M. The maximum M obtained indicates that the optimum WTE can be achieved at perfectly matched conditions. Here, the maximum WTE can be reached at a matching distance equal to 25 mm. Figure 10 shows the WTE alteration of both PLAs and PRLAs antennas for various distances. Even though the WTE for PRLA is lower than PLA at matching distance, WTE for PRLA has better stability than PLA. Frequency splitting phenomena has been reduced greatly by introducing reverse loop into PRLA. As a result, WTE for PRLA at closer distance from matching distance is higher than PLA.

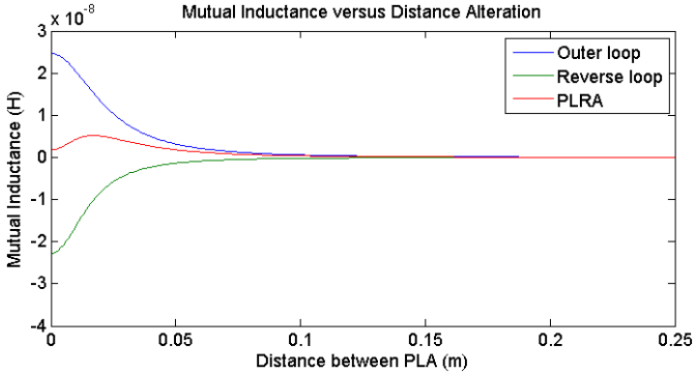

Figure 9. Total mutual inductance, M versus distance between PRLAs

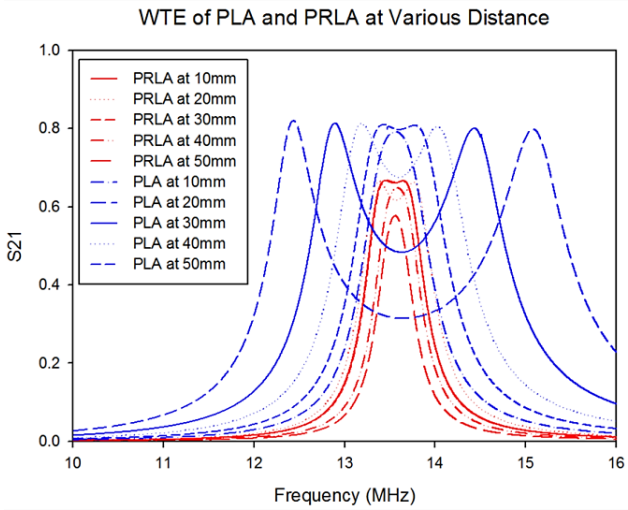

Figure 10. Transfer efficiency with distance alteration

Figure 11 compares the WTE performance of the PRLA and conventional PLA as the operating distance is varied. Differences in capacitor values within a 5% tolerance contribute to differences between the simulation and measurement results. Non-existent values for required capacitors in the market also led to this dissimilarity.

However, there is acceptable agreement between the measured and simulated profiles of WTE. Overall, the PLRA is shown to stabilise the WTE at closer distances. An improvement of 150% for S21 at a distance of 10mm is recorded. In addition, the PLRA is able to maintain S21 over 0.5 at a greater distance than the conventional PLA. PLA has S21 larger than 0.5 from 25 mm to 75 mm while PRLA manage to maintain S21 above 0.5 from 0 up to 60 mm, which produce range improvement of 20%.

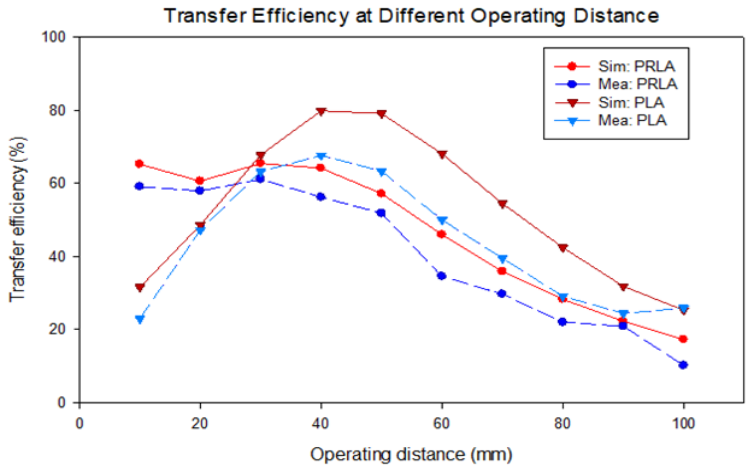

Figure 11. Transfer efficiency with varied distances

4. Conclusion

WTE can be stabilised over shorter coupling distances by using the reverse loop technique at a closer distance. By controlling the increase in mutual inductance between a pair of coupled antennas at shorter distances, the alteration of WTE is reduced. This leads to an improvement in the stability of WET.

Acknowledgements

The authors would like to thank Universiti Teknikal Malaysia Melaka (UTeM) for supporting this research work under the grant PJP/2017/FKEKK/HI13/S01541. This research also was supported by Universiti Teknologi Malaysia.

References

[1] Shoki H. *Issues and initiatives for practical deployment of wireless power transfer technologies in Japan*. Proceedings of the IEEE. 2013; 101(6): 1312–1320.
[2] http: //www.mouser.com/pdfdocs/... ...STMicroelectronicsIntroductiontoNFC.pdf. Accessed 21st June 2016 at 4:00 pm.
[3] Strommer E, Jurvansuu M, Tuikka T, Ylisaukko-Oja A, Rapakko H, Vesterinen J. *NFC-Enabled Wireless Charging*. 2012 4th International Workshop on Near Field Communication (NFC). 2012: 36–41.
[4] Jolani F, Yu Y, Chen Z. *A Novel Planar Wireless Power Transfer System with Strong Coupled Magnetic Resonances*. 2014 IEEE International Wireless Symposium (IWS). 2014: 1-4.
[5] Mori K, Lim H, Iguchi S, Ishida K, Takamiya M, Sakurai T. Positioning-free resonant wireless power transmission sheet with staggered repeater coil array (SRCA). *IEEE Antennas and Wireless Propagation Letter*. 2013; 11: 1710-1713.

[6] Lee WS, Oh KS, Yu JW. Distance-insensitive wireless power transfer and near-field communication using a current-controlled loop with a loaded capacitance. *IEEE Transactions on Antennas and Propagation*. 2014; 62(2): 936-940.
[7] Mai R, Zhang Y, Dai R et al. A three-coil inductively power transfer system with constant voltage output. *Energies Journal*. 2018; 11(3): 637-649.
[8] Ricketts DS, Chabalko MJ, Hillenius A. *Optimization of Wireless Power Transfer for Mobile Receivers Using Automatic Digital Capacitance Tuning*. 2013 European Microwave Conference (EuMC). 2013; 1: 515-518.
[9] Kim Y, Lim S. *High efficient misaligned wireless power transfer using magnetic resonant coupling and additional capacitor*. Asia-Pacific Microwave Conference Proceedings, APMC. 2012: 1049-1051.
[10] Ahn D, Hong S. Wireless Power Transfer Resonance Coupling Amplification by Load-Modulation Switching Controller. *IEEE Transactions on Industrial Electronics*. 2014; 62(2): 898-909.
[11] Lee WS, Son WI, Oh KS, Yu JW. Contactless energy transfer systems using antiparallel resonant loops. *IEEE Transactions on Industrial Electronics*. 2011; 60(1): 350-359.
[12] Zhong WX, Zhang C, Liu X, Hui SR. A Methodology for Making a 3-Coil Wireless Power Transfer System More Energy Efficient Than a 2-Coil Counterpart for Extended Transmission Distance. *IEEE Transactions on Power Electronics*. 2014; 30(2): 933-942.
[13] Imura T, Hori Y. Maximizing Air Gap and Efficiency of Magnetic Resonant Coupling for Wireless Power Transfer Using Equivalent Circuit and Neumann Formula. *IEEE Transactions on Industrial Electronics*. 2011; 58(10): 4746-4752.
[14] Beh TC, Kato M, Imura T, Oh S, Hori Y. Automated impedance matching system for robust wireless power transfer via magnetic resonance coupling. *IEEE Transactions on Industrial Electronics*. 2012; 60(9): 3689–3698.
[15] Park J, Tak Y, Kim Y, Kim Y, Nam S. Investigation of adaptive matching methods for near-field wireless power transfer. *IEEE Transactions on Antennas and Propagation*. 2011; 59(5): 1769–1773.
[16] Sample AP, Waters BH, Wisdom ST, Smith JR. *Enabling seamless wireless power delivery in dynamic environments*. Proc. IEEE. 2013; 101(6): 1343–1358.
[17] Sample AP, Meyer DT, Smith JR. Analysis, experimental results, and range adaptation of magnetically coupled resonators for wireless power transfer. *IEEE Transactions on Industrial Electronics*. 2010; 58(2): 544–554.
[18] Jang BJ, Lee S, Yoon H. Hf-Band Wireless Power Transfer System: Concept, Issues, and Design. *Prog. Electromagn. Res*s. 2012; 124: 211–231.
[19] Trigui A, Hached S, Mounaim F, Ammari AC, Sawan M. Inductive Power Transfer System with Self-Calibrated Primary Resonant Frequency. *IEEE Trans. Power Electron.* 2015; 30(11): 6078–6087.
[20] Zhao C, Wang Z, Du J, Wu J, Zong S, He X. *Active resonance wireless power transfer system using phase shift control strategy*. Appl. Power Electron. Conf. Expo. (APEC). 2014 Twenty-Ninth Annu, IEEE. 2014: 1336–1341.
[21] Hu W, Zhou H, Deng Q, Gao X. *Optimization algorithm and practical implementation for 2-coil wireless power transfer systems*. 2014 Am. Control Conf. 2014: 4330–4335.
[22] Roland M, Witschnig H, Merlin E, Saminger C. *Automatic impedance matching for 13.56 MHz NFC antennas*. Proc. 6th Int. Symp. Commun. Syst. Networks Digit. Signal Process-CSNDSP 08. 2008: 288–291.
[23] Witschnig H, Roland M, Gossar M, Enzinger H. Parameter characterisation and automatic impedance matching of 13.56 MHz NFC antennas. *Elektrotechnik und Informationstechnik*. 2009; 126(11): 415–422.
[24] Yilmaz M, Krein PT. Review of battery charger topologies, charging power levels, and infrastructure for plug-in electric and hybrid vehicles. *IEEE Trans. Power Electron*. 2013; 28(5): 2151–2169.
[25] Covic GA, Boys JT. *Inductive Power Transfer*. Proc. IEEE. 2013; 101(6): 1276–1289.
[26] Kurs A, Karalis A, Moffatt R, Joannopoulos JD, Fisher P, Soljačić M. Wireless power transfer via strongly coupled magnetic resonances. *J. Science*. 2007; 317(5834): 83–86.
[27] Mayordomo I, Dräger T, Spies P, Bernhard J, Pflaum A. *An overview of technical challenges and advances of inductive wireless power transmission*. Proc. IEEE. 2013; 101(6): 1302–1311.
[28] Wei X, Wang Z, Dai H. A Critical Review of Wireless Power Transfer via Strongly Coupled Magnetic Resonances. *Energies Journal.* 2014: 4316-4341.
[29] Raju S, Wu R, Chan M, Yue CP. Modeling of Mutual Coupling Between Planar Inductors in Wireless Power Applications. *IEEE Transactions on Power Electronics*. 2013; 29(1): 481–490.